Journal of Archaeological Science 36 (2009) 1745–1757

Contents lists available at ScienceDirect

Journal of Archaeological Science

journal homepage: http://www.elsevier.com/locate/jas

Slag inclusions in iron objects and the quest for provenance: an experiment and a case study

Eleanor Blakelock*, Marcos Martinón-Torres [1], Harald A. Veldhuijzen [1], Tim Young [2]

Division of Archaeological, Geographical and Environmental Sciences, University of Bradford, BD7 1DP Bradford, West Yorks, United Kingdom

ARTICLE INFO

Article history:
Received 5 May 2008
Received in revised form
26 March 2009
Accepted 29 March 2009

Keywords:
Iron
Slag inclusions
Provenance
Experimental archaeology
Hammeh
Beth-Shemesh

ABSTRACT

Slag inclusions are found within most archaeological bloomery iron artefacts and are remainders of slag created during the smelting and smithing processes. Although they are widely believed to provide data with the potential for provenancing iron artefacts, previous slag inclusion studies have mostly proven inconclusive. The main aim of the work reported here is to analyse experimental smelting and smithing assemblages (including ore, furnace lining, fuel and slag), to compare these to slag inclusions in the resulting bloom and worked objects, and then explore the relationships between ore, slag and slag inclusions. This study has revealed that the composition of slag inclusions most closely relates to the smelting slag produced, whereas provenance to a specific ore would be difficult due to the chemical variability derived from furnace lining, fuel and any fluxes used. Some compounds in the slag inclusions are particularly affected during smithing of the artefact, i.e. those present in the sand flux and fuel used. However, trends are observed in the K_2O/MgO, MnO/SiO_2, Al_2O_3/SiO_2, Al_2O_3/MgO, Al_2O_3/K_2O and Al_2O_3/CaO ratios that allow comparison between slag inclusions and smelting slag in these experiments, and may therefore be used during other provenancing attempts. The knowledge gained from the experimental assemblages was subsequently applied to an archaeological case study, examining objects from the 900 Cal BC smithing site of Tel Beth-Shemesh, Israel and the 930 Cal BC smelting site of Tell Hammeh, Jordan. The analyses suggest that none of the artefacts examined derived from the Hammeh smelting system.

1. Introduction

Iron has been a valuable commodity since the Iron Age and was utilised to create an array of objects. The main method of smelting iron ores in premodern times was the so-called "direct" or "bloomery" method, in which the ore is processed in a furnace with carbon-rich fuel at temperatures around 1200 °C. In this process the iron never reaches the molten state, but as iron oxides are reduced they coalesce as a solid mass of metal or "bloom". This bloom can subsequently be refined and shaped into the required forms by hot working or smithing (Pleiner, 2000).

The main by-product of smelting is an iron oxide-rich slag, formed predominately by the reaction between iron oxide and silica; other impurities in the ore are often incorporated into the slag during the process, together with molten material from the technical ceramics (e.g. tuyères and furnace lining) and fuel ash (Bachmann, 1982; Buchwald and Wivel, 1998; Crew, 2000; McDonnell, 1987; Paynter, 2006; Pleiner, 2000; Rostoker and Bronson, 1990; Tylecote, 1986; Veldhuijzen, 2005b). A range of slag morphologies can be produced during the smelting of iron, depending on the raw materials, furnace structure and operating parameters; often several of these form in the same smelt. These may include furnace bottom slag, furnace slag, tap slag, ceramic-rich slag, and a glassy slag that forms around the bloom (Allen, 1988; McDonnell, 1986; Veldhuijzen, 2005a; Veldhuijzen and Rehren, 2007). Analytical studies of smelting slag show a systematic and highly repetitive pattern in slag composition, with most smelting slags plotting in the fayalitic region of the $FeO–Al_2O_3–SiO_2$ ternary phase diagram. Even so, small differences in the final composition are direct consequences of human decisions regarding furnace design, raw materials and engineering parameters (Rehren et al., 2007).

During bloomery smelting, the solid iron bloom, although much denser than the slag, does not sink to the base of the furnace. Instead it attaches itself to the furnace wall just below tuyère level. As the bloom forms, particles of slag and charcoal become incorporated, therefore primary smithing is carried out by hammering the bloom, typically while still hot, to remove adhering slag and expel inclusions of slag and charcoal (Hedges and Salter, 1979; McDonnell,

* Corresponding author.
E-mail address: eleanor.blakelock@blueyonder.co.uk (E. Blakelock).
[1] UCL Institute of Archaeology, 31-34 Gordon Square, WC1H 0PY London, United Kingdom.
[2] GeoArch, Unit 6, Western Industrial Estate, Caerphilly, Wales CF83 1BQ,, United Kingdom.

0305-4403/$ – see front matter © 2009 Elsevier Ltd. All rights reserved.
doi:10.1016/j.jas.2009.03.032

1991; Pleiner, 2006; Serneels and Perret, 2003), simultaneously consolidating the metal into more compact and manageable billet or bar. Secondary smithing is the operation where the resulting metal billet or bar is shaped into a finished product, by repeatedly heating the iron in a hearth and hammering it on an anvil. To weld pieces of iron together it is vital that the metal is heated to a temperature at which it is soft but not molten (c. 1100 °C), and that there is a 'clean' metal surface to allow diffusion bonding. However, during secondary smithing large amounts of metal are lost due to oxidisation, with an oxidised crust forming on the surface of the metal worked. This can be removed by hammering (resulting in hammerscale), and in addition a flux (e.g. siliceous sand) may be used to remove the iron oxide in the form of fayalitic slag (McDonnell, 1987; Pleiner, 2006; Serneels and Perret, 2003).

The expulsion of slag during the primary and secondary smithing processes was never perfect, therefore primary slag inclusions are commonly found in iron artefacts. New, secondary, slag inclusions may also be introduced into the iron artefact during later stages in production, for example when folding or welding whilst smithing (Fig. 1).

Various studies have investigated whether the geological origin of an archaeological iron artefact can be determined using the chemical composition of the slag inclusions (hereafter, SI) within the object (Buchwald and Wivel, 1998; Coustures et al., 2003; Dillmann and L'Héritier, 2007; Hedges and Salter, 1979; Høst-Madsen and Buchwald, 1999). The underlying assumption of earlier studies was that the variability in ore compositions should be reflected in the chemistry of SI (Hedges and Salter, 1979). More recently, researchers have began to refine these approaches by noting that other factors such as fuel ash, fluxes and furnace lining, together with variable operating parameters, do contribute significantly to slag formation, and that therefore SI in objects should be related to specific "smelting systems" rather than generic geological ores (Dillmann and L'Héritier, 2007; Paynter, 2006). This has led some to compare compositional data between SI and smelting slags (rather than ores alone), hoping to identify better matches (Buchwald and Wivel, 1998; Coustures et al., 2003). Most of these provenancing attempts, however, have been unconvincing or only partly conclusive, and their interpretation of the data remains speculative.

We believe that a major limitation of previous work is that the chemical behaviour of different elements involved in the smelting and smithing systems has been assumed rather than tested. For example, Coustures et al. (2003) have spoken of "incompatible trace elements", that are preferentially concentrated in the liquid phase and are therefore likely to end up in the slag and SI rather than the metal itself, and Dillmann and L'Héritier (2007) focused on what they term "non-reduced compounds". However, the chemical relationships between ores, furnace material and fuel ash, and their impact on the resulting SI, as well as the changing composition of SI during smithing, have not been investigated in detail. Although some of these studies analysed SI in experimentally produced iron objects, they did not attempt to relate these to the relevant raw materials and slags. Hence, any ascription of an iron object to a source based on SI remained tentative rather than conclusive.

The research reported here aims to contribute to SI provenancing studies by drawing primarily on the study of experimental material. We present the analyses of complete assemblages created from three experimental iron smelts, to characterise the different slag produced, as well as the metal and SI found in the bloom. The SI from the primary and secondary smithing of the bloom to billet and/or bar are also studied along with the smithing slag produced, and samples of the ore, charcoal and clays employed. The data are then explored to assess the relative importance of ore, fuel and fluxes in the composition of slag and SI, as well as constraints and patterns that may be used to model their compositional changes during smelting and smithing. The ultimate ambition is to further test the validity of SI provenance studies and to try to demarcate precise analytical or data processing criteria that might facilitate future work. Following the presentation of the experiments, our observations are applied to an archaeological case study from Iron Age contexts in the Near East.

2. Methodology and data processing

A series of smelting experiments were carried out by Tim Young over several summers from 1998 to 2004 at the Museum of Welsh Life, near Cardiff. Specific details of each of the three experiments selected for the present project are given in the next section. In

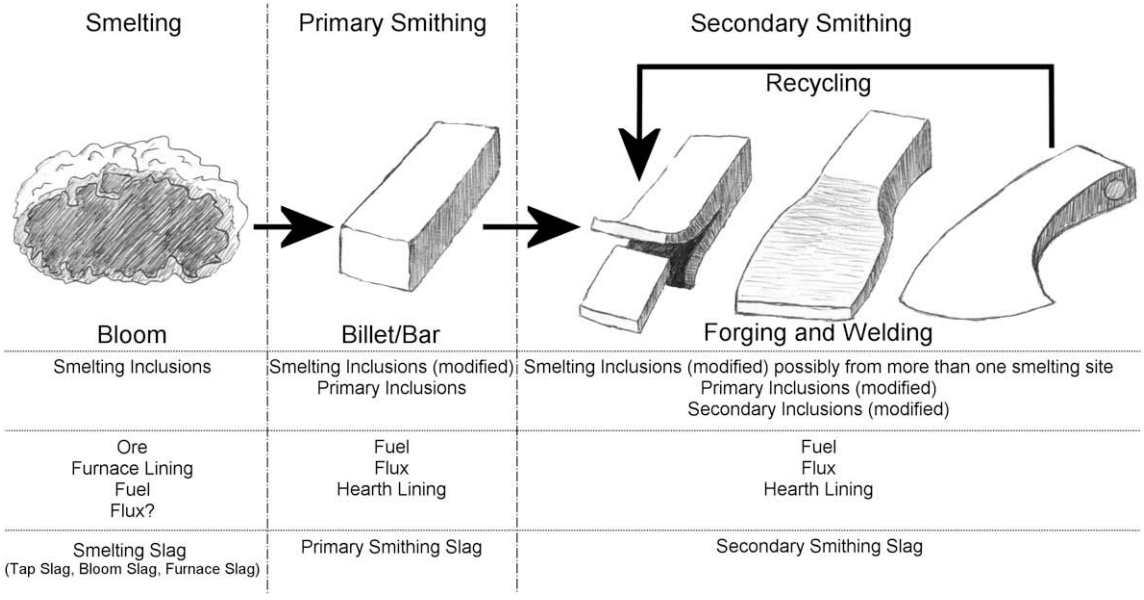

Fig. 1. Stages of production from bloom to artefact. Below each stage is a description of the types of slag inclusions present. Below that are the principal components involved in that stage that may affect the composition of the inclusions and then a description of the slag types formed (Blakelock, 2007, p. 24). Artefact sketches (apart from bloom) based on those from Buchwald (2005, p. 280).

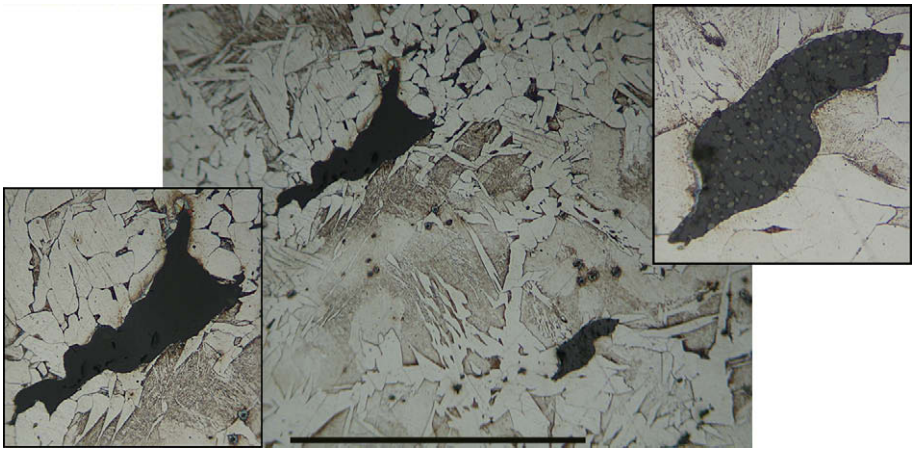

Fig. 2. Single- and multi-phased slag inclusions from the bar produced in experiment 1, centre picture taken using plain polarised light at ×100 magnification where the scale bar equals 0.5 mm. Close ups of slag inclusions insets taken at ×200 (left) and ×500 (right).

general, a number of samples were removed from each experimental assemblage. Two samples of each type of slag created were chosen, i.e. tap slag, ceramic-rich slag, bloom slag and smithing slag. Two samples of metal were removed from each of the blooms and one sample from each billet/bar. The samples were then mounted in a two-component epoxy resin, ground and polished using diamond pastes to a 1 μm finish. The iron samples were examined using a metallographic microscope to study the nature and distribution of SI, and the slag samples were examined to obtain a first assessment of their microstructure. The polished blocks were subsequently carbon coated for SEM–EDS analyses. After SI analyses by SEM–EDS, iron samples had the carbon coating removed and were etched in using a 2% nital solution for further metallographic study.

The composition of the slag and SI was determined using an Oxford Instruments energy dispersive spectrometer attached to a Philips XL30 scanning electron microscope (SEM–EDS). Both backscatter and secondary electron modes were used to assess the microstructure of each sample. Analytical parameters were kept constant at an accelerating voltage of 20 kV, processing time of 5 and ≈40% deadtime. When analysing the slag, 15 separate areas of at least 300 by 300 μm were analysed for bulk composition, in addition to spot analyses of separate phases when appropriate. In SI analyses, at least 25% and preferably 50% of the inclusion area was probed. In addition, only inclusions greater than 10 × 10 μm were analysed to reduce the risk of localised concentration effects, noted during Dillmann and L'Héritier's (2007) study . For each analysis of a SI, the number and type of phases present (Fig. 2), shape, approximate surface area, and relative area analysed were recorded. Overall, approximately 30–50 SI were analysed per object, except for particularly corroded archaeological objects where fewer SI were left in the polished sample. All the compositional data are reported in this paper as weight percentages (wt%), combined with oxygen by stoichiometry and normalised to 100%, to account for fluctuations in beam intensity and to facilitate comparisons. However, average analytical totals prior to normalisation are also reported. Instrumental precision and accuracy were tested through repeated analyses of reference basalts from the US Geological Survey (Table 1). The results are generally good, with the exceptions of soda (which will not be employed in our study), and magnesia (which appears systematically underestimated by ~20% relative). All the patterns derived from our data comparisons are based on differences larger than the ranges of analytical uncertainty identified.

Our analyses and data processing protocols draw on the recent recommendations made by Dillmann and L'Héritier (2007) following their extensive work on SI in medieval architectural iron, but our approach differs from theirs in certain aspects. A particularly useful point was their emphasis on the fact that, notwithstanding the chemical variability of different SI within a single object, the ratios of the "non-reduced compounds" (NRCs) tend to remain broadly constant for any given object (these compounds are

Table 1
Results from precision and accuracy tests performed on geochemical reference materials from the US Geological Survey (USGS). The four rows for each reference material present the certified values from the USGS ('reference'), the average results for 12 SEM–EDS measurements of 100 by 100 μm areas on the reference materials prepared as polished blocks ('analysed'), the standard deviation for those 12 measurements (STDev), and the difference between analysed and reference values for each compound (δ). All values are in wt%, and SEM–EDS data have been normalised to 100%. Below detection limits = bd.

		Na_2O	MgO	Al_2O_3	SiO_2	P_2O_5	K_2O	CaO	TiO_2	MnO	FeO
BIR-1	Reference	1.82	9.70	15.5	48.0	0.02	0.03	13.3	0.96	0.18	10.2
	Analysed	1.17	7.79	13.7	49.1	bd	bd	14.9	1.17	0.19	11.9
	STDev	0.08	0.05	0.09	0.20			0.15	0.04	0.07	0.18
	δ	−0.65	−1.91	−1.76	1.17			1.62	0.21	0.01	1.72
BHVO-2	Reference	2.22	7.23	13.5	49.9	0.27	0.52	11.4	2.73	0.17	11.1
	Analysed	1.39	5.79	11.9	51.1	0.27	0.57	12.7	3.16	0.19	12.9
	STDev	0.10	0.08	0.13	0.23	0.12	0.03	0.14	0.10	0.04	0.14
	δ	−0.83	−1.44	−1.57	1.23	0.00	0.05	1.30	0.43	0.03	1.81
BCR-2	Reference	3.16	3.59	13.5	54.1	0.35	1.79	7.12	2.26	0.20	12.4
	Analysed	1.99	2.82	11.9	55.7	0.37	2.01	7.93	2.73	0.24	14.3
	STDev	0.05	0.07	0.12	0.20	0.13	0.07	0.11	0.14	0.07	0.16
	δ	−1.17	−0.77	−1.62	1.59	0.02	0.22	0.81	0.47	0.04	1.93

Table 2
Chemical composition of the raw materials used in the experimental smelts including the two different ore sources used.

	Na_2O	MgO	Al_2O_3	SiO_2	P_2O_5	SO_3	K_2O	CaO	TiO_2	MnO	FeO	Total
Clay and brick[a]	0.8	1.6	25.7	57.5	0.4	0.2	5.0	1.0	1.0	0.1	6.6	86.7
Fuel ash[b]	1.8	6.8	0.3	2.2	7.2	bd	22.1	58.9	bd	0.5	0.3	90.6
Sishen ore[b]	0.1	0.1	0.8	1.4	0.1	bd	0.1	0.1	0.1	bd	97.2	88.9
Blaenavon ore[c]	0.3	3.1	4.3	12.8	0.4	0.1	0.7	1.4	0.1	1.0	75.7	107.2

[a] SEM–EDS bulk analysis.
[b] X-ray fluorescence (XRF) analysis carried out by Gary Thomas (Young, Pers. Comm.).
[c] Combined average from SEM–EDS and XRF analysis by Gary Thomas (Young, Pers. Comm.).
The total column gives the average analytical total prior to normalisation. Below detection limits = bd.

MgO, Al_2O_3, SiO_2, K_2O, CaO and TiO_2; we have included MnO when higher than 0.1%) (see also Buchwald and Wivel, 1998; Buchwald, 2005). Thus, when plotted on bivariate scatters, concentrations of NRC tend to show a linear distribution. Based on this, our comparison between compositions of SI and slags will mostly employ these ratios rather than average bulk compositions. Dillmann and L'Héritier (2007) go on to suggest that, for each object, "abnormal data" may be deleted from the NRC data bivariate plots in iterative steps, until the determination coefficient (R^2) for a regression line passing through zero is higher than 0.7. For some of our samples, however, this "data cleaning" process would have required removing up to 50% of the measurements, incurring a high risk of artificially distorting the patterns observed. Thus we have decided to plot our full datasets and assess their relationships qualitatively rather than quantitatively, so that the chemical diversity of the SI was shown rather than erased. However, statistical tests such as the two-tailed *t*-test have been used to determine whether patterns and observations in the data are statistically significant. For this study we consider any $p < 0.05$ as significant and $p > 0.05$ as insignificant.

Whilst most previous studies have used normal average compositions of all the SI from a given object, Dillmann and L'Héritier (2007) propose the use of a "weighted average composition", where the contribution of a given SI to the final average is a function of its size. In the present study, we avoided small inclusions, and the vast majority of the SI analysed were of a similar size for each object, so when the "weighted average" composition was calculated the resulting values were typically within one standard deviation of the original "un-weighted average". Thus, whilst acknowledging the usefulness of this formula for potentially more heterogeneous objects, we shall not be using it here.

3. The experimental smelts and the resulting slag

The experimental programme conducted at the Museum of Welsh Life was designed to investigate the smelting of iron ores like those exploited in the region in antiquity. The large slag-tapping bloomery furnace used is a reconstruction of what is believed to be a typical type of furnace used in the area throughout the first millennium AD, and also based on the successful furnaces constructed by Peter Crew (Crew, 1991). The three assemblages studied in this project were from experiments 26, 23 and 17. However for simplicity sake, they will here be termed experiments 1, 2 and 3 (abbreviated XP1, XP2 and XP3), respectively.

The chemical composition of the raw materials used during the experiments is shown in Table 2. The furnace and smithing hearth were constructed from raw clay dug on the site, without additional binders or temper. The charcoal fuel used was oak, which was particularly rich in lime, potash, magnesia and phosphate. Quartz sand was used as a flux during smithing to prevent the iron from cracking. These materials were identical in all three experiments, but different ores were employed. In experiments 1 and 2, a high-grade Sishen ore (South African haematite) was used, whilst experiment 3 involved a sideritic ironstone from Blaenavon.

3.1. Experiment 1

Experiment 1 was chosen as it represented the full processing of iron from bloom through billet to bar, with samples from all stages in between also represented. It also provided a complete assemblage of smelting and smithing slags. The overall average compositions of the four different slag types from this experiment are presented in Table 3. As would be expected from their morphology and the processes involved each slag had its own distinct composition. The two most similar slag types are the tap slag and the bloom slag (i.e. slag directly attached to the bloom, removed with a wooden mallet before smithing). Both of them have a composition typical of most archaeological tap slag, although the bloom slag is depleted in iron oxide, which was also noted in its microstructure by the absence of wüstite (Fig. 3). As expected, the ceramic-rich slag, dominated by molten furnace lining, was characterised by a much higher SiO_2/FeO ratio, whilst the smithing slag showed generally higher values for MgO, K_2O, P_2O_5 and CaO, a likely result from a higher fuel ash contribution.

3.2. Experiment 2

Previous research has confirmed that the slag produced using similar, if not identical, raw materials and conditions should be very close in composition (Buchwald and Wivel, 1998; Bullas, 1995; Dillmann and L'Héritier, 2007; Høst-Madsen and Buchwald, 1999; Paynter, 2006). Therefore, since experiment 2 employed the same raw materials and operating parameters as experiment 1, we can assume that the slag would be similar. A single bloom slag fragment

Table 3
Normalised average SEM–EDS data from the bulk analysis of different types of slag from experiment 1 compared to the bloom slag from experiment 2. The total column gives the average analytical total prior to normalisation.

Experiment		Na_2O	MgO	Al_2O_3	SiO_2	P_2O_5	SO_3	K_2O	CaO	TiO_2	MnO	FeO	Total
1	Tap slag	0.5	0.7	7.2	29.5	0.4	0.1	1.5	3.8	0.2	0.1	55.8	91.1
	Bloom slag	0.6	0.9	9.8	45.6	0.5	0.2	2.6	5.2	0.5	0.1	33.8	105.9
	Ceramic-rich slag	1.2	1.9	8.1	65.8	0.8	0.1	2.6	5.7	0.5	0.2	12.9	108.7
	Smithing slag	0.7	1.7	9.3	33.6	1.1	0.2	4.0	7.0	0.3	0.1	41.9	108.2
2	Bloom slag	0.4	0.8	8.1	48.6	0.4	0.4	2.2	4.9	0.6	0.1	33.4	95.5

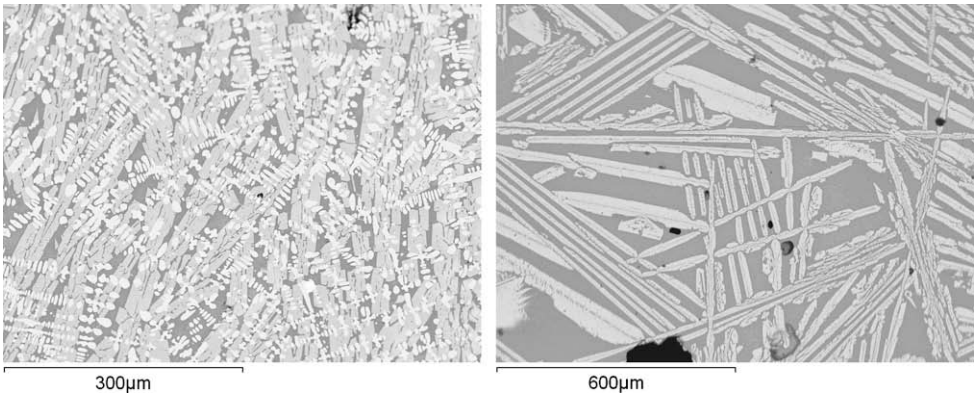

Fig. 3. Backscatter images of tap slag (left) and bloom slag (right) from experiment 1.

from this experiment was analysed, and its composition does compare well with the tap and bloom slag from experiment 1 (Table 3).

The main aim of including material from experiment 2, however, was to confirm that this compositional comparability also applied to the SI in the iron. As products of the same smelting and smithing systems, these SI should have the same NRC ratios, and ideally these should differ from those in object SI from experiment 3. The metal analysed from experiment 2 included a bloom fragment, part of the billet and a fragment of worked iron that fell off during working.

3.3. Experiment 3

This experiment not only used a different source of ore but also had slightly different smelting and smithing conditions, with a lower shaft smelting furnace, slower blow rates and a smaller smithing hearth. As with the other experiments, a range of slag types from this experiment were analysed. In addition, a sample of the final smithed bar was examined.

The average compositions of the three different slag types produced during experiment 3 are presented in Table 4. As in experiment 1, there were remarkable similarities between the tap and bloom slag, apart from the slightly lower FeO and higher CaO content in the latter. Overall, the most notable difference between these slags and those from experiment 1 is that all of the slag samples from experiment 3 contain small but significant levels of MnO, clearly derived from the ore, even if the ore contained only 1% MnO.

4. Slag inclusions in the experimental assemblages

The analysis of SI revealed that a range of inclusion types could be present. The majority of inclusions identified were either multi-phased, with fayalite in a glass matrix, or just single-phased with a glassy appearance (Fig. 2). However, occasionally other types of inclusions were noted, including multi-phased inclusions with fayalite and wüstite in a glass matrix and occasionally multi-phased inclusions which consisted almost entirely of magnesia-rich olivines in an alkali-rich glass. As expected, the composition varied between the different SI types, but most often they had comparable NRC ratios. In some cases (Fig. 4) the SI for the same object form distinct compositional clusters, with billets SI (having undergone smelting plus one smithing stage) clumping in two clusters, and bars SI (with an extra smithing stage) plotting in three. This pattern might reflect changing frequencies of inclusion types between smithing phases – an aspect deserving further investigation. It was clear, however, that both multi- and single-phased inclusions are found at weld lines, and thus it is unlikely that any single SI type can be easily disregarded as created during the smithing process. Therefore, all inclusion types will be considered during the discussion without discerning between types. The average chemical compositions of the different SI types analysed in the experimental blooms, billets and bars are shown in Tables 5–7.

The presentation and discussion of data on the SI from experimental assemblages will be divided into three sections. First, we will compare the SI in the objects from different experiments, to test whether different "smelting systems" can be discerned on the basis of object SI. Second, the SI in objects will be compared to those in the blooms from the relevant experiments. Thirdly, the composition of object SI will be compared to those of the relevant smelting slag, trying to identify any patterns that would allow correlations between archaeological smelting slag and objects based on SI analyses. The final section will utilise the knowledge gained from the analyses of the experimental assemblages in an archaeological case study.

4.1. SI in billets and bars

Fig. 4 shows several plots of NRC ratios for the billets and bar samples produced in the various experiments. As previously noted by Dillmann and L'Héritier (2007), these ratios tend to display a broad linear distribution for each object, even though, as noted above, either a broader scatter or a tight clustering of the data may obscure these correlations.

It is immediately apparent that the XP3 bar shows some clearly distinct NRC ratios, which is consistent with its origins in a different smelting system. This is particularly clear in the SiO_2/MnO ratio, derived from the fact that the ore used in experiment 3 was the only one containing any significant levels of MnO. The K_2O/MgO

Table 4
Normalised average SEM–EDS data from the bulk analysis of different types of slag from experiment 3. The total column gives the average analytical total prior to normalisation.

	Na_2O	MgO	Al_2O_3	SiO_2	P_2O_5	SO_3	K_2O	CaO	TiO_2	MnO	FeO	Total
Tap slag	0.4	2.3	8.5	37.0	0.7	0.3	2.0	4.9	0.4	0.9	42.5	106.9
Bloom slag	0.4	3.0	8.4	42.9	0.7	0.2	2.8	8.6	0.5	1.0	31.4	94.5
Smithing slag	0.3	4.2	6.9	30.2	0.5	0.4	1.4	2.5	0.2	1.1	52.2	95.6

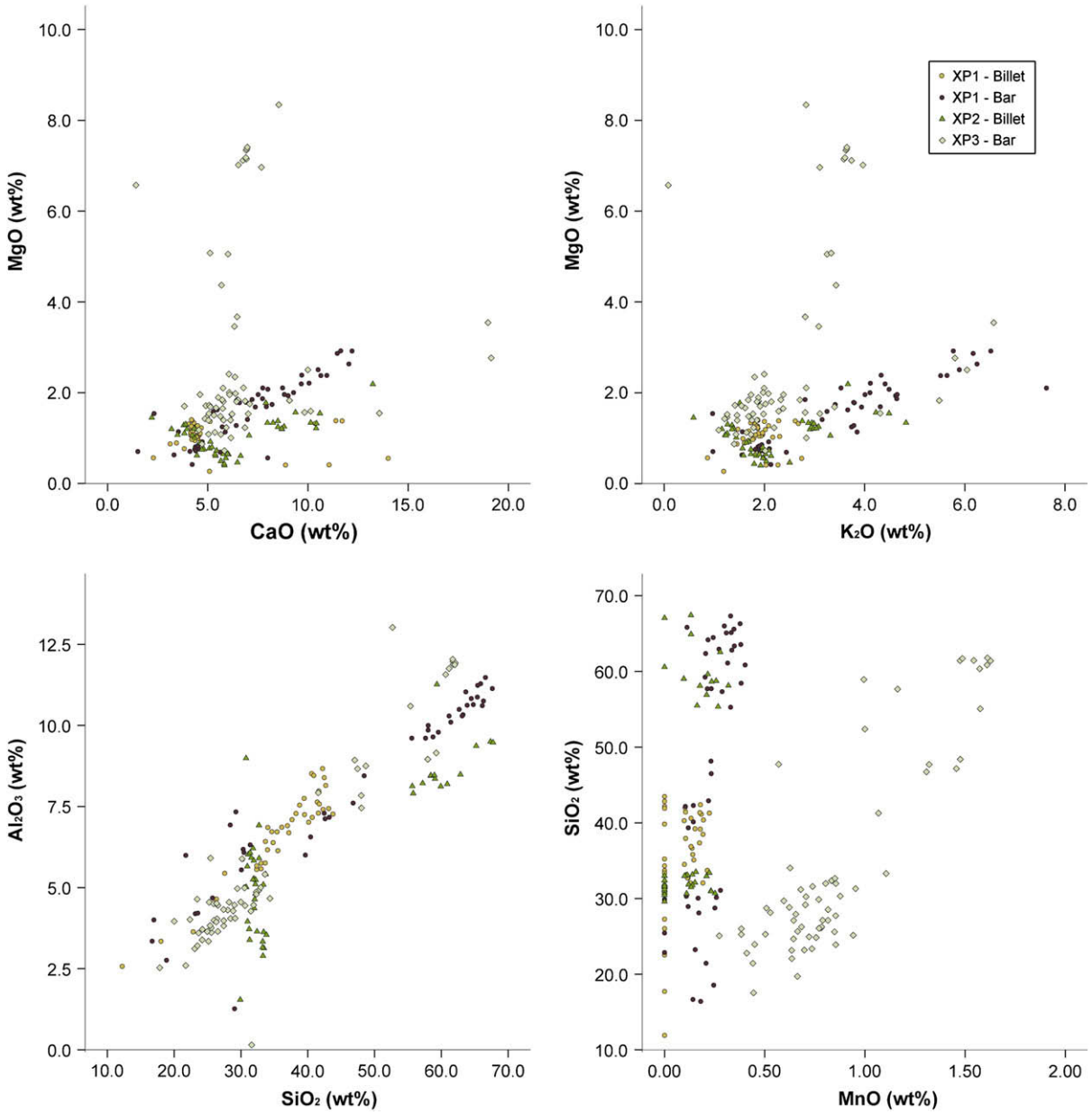

Fig. 4. Bivariate plots of non-reduced compounds (NRC) in SI in the iron objects from the three experiments.

Table 5
Normalised average SEM–EDS data from the analysis of the different types of SI found in the iron from experiment 1. The total column gives the average analytical total prior to normalisation.

	Phases		Na_2O	MgO	Al_2O_3	SiO_2	P_2O_5	SO_3	K_2O	CaO	TiO_2	MnO	FeO	Total
Bloom	Glassy	Avg	0.8	1.6	12.1	66.7	0.7	0.2	3.9	6.4	0.6	0.2	6.7	111.9
		STDev	*0.1*	*0.5*	*0.9*	*4.0*	*1.6*	*0.1*	*1.1*	*1.6*	*0.2*	*0.1*	*4.6*	
	Multi-phased	Avg	0.6	1.0	8.8	49.8	2.9	0.3	2.4	3.9	0.5	0.1	29.6	103.8
		STDev	*0.2*	*0.4*	*2.1*	*9.3*	*2.5*	*0.2*	*1.3*	*1.9*	*0.2*	*0.1*	*14.3*	
Billet	Glassy	Avg	0.6	1.1	7.3	38.8	0.7	0.2	1.8	4.2	0.4	0.1	44.6	106.6
		STDev	*0.1*	*0.2*	*1.2*	*5.5*	*0.2*	*0.1*	*0.3*	*0.5*	*0.1*	*0.1*	*7.5*	
	Multi-phased	Avg	0.5	0.9	5.8	31.4	3.4	1.1	2.0	7.1	0.2	0.1	47.4	110.5
		STDev	*0.1*	*0.4*	*1.3*	*6.7*	*3.0*	*1.2*	*0.5*	*3.7*	*0.1*	*0.1*	*11.2*	
Bar	Glassy	Avg	0.6	2.2	10.7	63.6	0.1	0.1	4.9	9.5	0.7	0.3	7.2	99.1
		STDev	*0.1*	*0.4*	*0.5*	*2.8*	*0.1*	*0.1*	*0.9*	*1.7*	*0.1*	*0.1*	*3.7*	
	Multi-phased	Avg	0.4	1.2	6.2	34.3	1.8	1.0	2.7	5.3	0.4	0.2	46.5	99.2
		STDev	*0.1*	*0.5*	*2.1*	*12.2*	*1.9*	*1.2*	*1.4*	*1.8*	*0.2*	*0.1*	*15.9*	

Table 6
Normalised average SEM–EDS data from the analysis of the different types of SI found in the iron from experiment 2. The total column gives the average analytical total prior to normalisation.

	Phases		Na_2O	MgO	Al_2O_3	SiO_2	P_2O_5	SO_3	K_2O	CaO	TiO_2	MnO	FeO	Total
Bloom	Glassy	Avg	0.6	1.1	10.6	59.3	2.1	0.4	3.8	5.0	0.8	0.2	15.8	106.0
		STDev	*0.2*	*0.6*	*3.2*	*10.1*	*3.1*	*0.3*	*1.9*	*2.1*	*0.7*	*0.1*	*9.4*	
	Multi-phased	Avg	0.6	0.6	7.5	49.4	2.1	1.3	2.9	3.9	0.5	0.1	31.0	91.4
		STDev	*0.4*	*0.2*	*1.3*	*9.0*	*1.1*	*1.1*	*1.7*	*1.9*	*0.2*	*0.1*	*10.4*	
Worked Bloom	Glassy	Avg	0.6	1.0	7.4	64.0	1.4	0.1	4.5	2.9	0.6	0.1	17.3	103.2
		STDev	*0.2*	*0.2*	*1.0*	*7.7*	*1.1*	*0.1*	*2.4*	*0.9*	*0.1*	*0.1*	*7.1*	
	Multi-phased	Avg	0.3	1.1	4.4	37.4	1.9	0.2	3.9	6.3	0.3	0.1	44.0	101.5
		STDev	*0.1*	*0.2*	*0.9*	*5.9*	*1.1*	*0.1*	*1.3*	*1.5*	*0.1*	*0.1*	*7.3*	
Billet	Glassy	Avg	0.4	1.1	6.9	46.6	0.7	0.2	2.5	7.3	0.5	0.1	33.4	107.8
		STDev	*0.2*	*0.4*	*2.4*	*14.4*	*0.7*	*0.1*	*1.0*	*2.4*	*0.2*	*0.1*	*19.7*	
	Multi-phased	Avg	0.3	0.8	4.8	31.6	0.8	0.2	1.6	4.7	0.3	0.1	54.8	103.4
		STDev	*0.1*	*0.3*	*1.2*	*0.8*	*0.4*	*0.1*	*0.4*	*1.0*	*0.1*	*0.1*	*3.1*	

Table 7
Normalised average SEM–EDS data from the analysis of the different types of SI found in the iron bar from experiment 3. The total column gives the average analytical total prior to normalisation.

	Phases		Na_2O	MgO	Al_2O_3	SiO_2	P_2O_5	SO_3	K_2O	CaO	TiO_2	MnO	FeO	Total
Bar	Glassy	Avg	0.3	5.7	10.3	55.1	0.5	0.2	3.9	8.3	0.7	1.3	13.5	105.9
		STDev	*0.1*	*1.9*	*1.8*	*7.0*	*0.6*	*0.2*	*1.1*	*4.2*	*0.1*	*0.3*	*7.9*	
	Multi-phased	Avg	0.2	1.9	4.2	27.8	3.0	0.8	1.9	5.5	0.2	0.7	53.8	108.7
		STDev	*0.1*	*1.1*	*1.1*	*4.5*	*1.9*	*1.2*	*0.7*	*1.2*	*0.1*	*0.2*	*4.7*	

ratio also shows a distinct signature for XP3 (Table 8), which must also be related to the higher levels of MgO and K_2O in the ore used for this experiment (Table 2). It is important to note, however, that the Al_2O_3/SiO_2 ratio remains fairly constant for all of the objects analysed, in spite of the different Al_2O_3/SiO_2 ratio in the ores employed. A *t*-test confirmed this observation revealing that the average Al_2O_3/SiO_2 ratio for the billet and bar in XP1 was not significantly different to the bar from XP3 ($t(190)1.54$, $p = 0.125$). We can only hypothesise that this is due to variable ceramic contributions to the slag formation in the two experiments, which may mask their respective signatures. Although this ratio in SI has been used previously to ascribe iron objects to different regions (e.g. Buchwald and Wivel, 1998), the present experiments indicate that such approaches should be regarded with caution, and ideally employed only in combination with other NRC ratios.

Turning specifically to the objects from XP1 and XP2, these show clearly comparable NRC ratios, and could therefore be assigned to the same smelting system. Only in the MgO/CaO ratio do we see some separation between the billets and bar from these experiments, especially noticeable in the higher MgO/CaO ratio in the bar. This may be due to the fact that the SI in the bar, having been subjected to a longer smithing process, may have taken up more fuel ash contamination. Overall, it is worth stressing that the ore used for both experiments 1 and 2 was very rich (Table 2), and that the chemical signature in the object SI is constrained by the fuel ash chemistry (i.e. alkali and alkali earth oxides) much more strongly than by the ore composition. This reinforces the idea that provenance attempts based on SI analyses may be better suited to relate objects to smelting systems (i.e. to metallurgical slag) than to geological sources (i.e. to ores alone) (see also Paynter, 2006). Furthermore, this observation highlights one potential problem: if two iron blooms from the same smelter are traded and subsequently worked by two smiths who employ different fuel, the resulting SI signatures are likely to be substantially different.

4.2. SI in objects and blooms

Comparison of slag inclusion sizes and shapes from the various stages from bloom to billet/bar has shown that there is little reduction in the number of SI nor is there a change in inclusion shape or size through the process. This suggests that, while some SI are expelled during smithing, others are created. As regards their compositions, Fig. 5 shows a comparison of some NRC ratios between the bloom and the objects produced in experiment 1, i.e. those belonging to the same smelting and smithing systems. A clear correlation between the bloom and object SI appears in the SiO_2/Al_2O_3 ratio. A *t*-test revealed no significant difference ($t(152) = -0.822$, $p = 0.413$) between the two sample means. This is somewhat surprising if one considers that the sand used as a flux during secondary smithing, consisting mostly of SiO_2, could have affected this ratio for the object SI. *t*-Tests also showed that there was no significant difference between SI in objects and blooms using the

Table 8
A tabular summary of the average relevant ratios for the experiment slag and object SI.

XP	Sample	Al_2O_3/SiO_2	Al_2O_3/MgO	Al_2O_3/K_2O	Al_2O_3/CaO	K_2O/CaO	K_2O/MgO	MgO/CaO	SiO_2/MgO	SiO_2/CaO	SiO_2/K_2O	MnO/SiO_2
1	Tap slag	0.245	10.80	4.82	1.89	0.39	2.25	0.182	43.9	7.7	19.7	0.003
1	Bloom	0.179	10.67	4.08	2.48	0.70	3.27	0.283	59.3	14.3	23.3	0.003
1	Billet	0.187	6.68	3.62	1.47	0.39	2.01	0.230	35.8	7.8	19.3	0.003
1	Bar	0.178	5.56	2.38	1.18	0.51	2.36	0.233	30.6	6.8	13.7	0.005
2	Bloom	0.174	18.71	3.29	2.85	1.02	7.88	0.223	101.3	15.3	20.2	0.003
2	Billet	0.150	6.71	2.85	0.96	0.34	2.38	0.181	43.3	6.8	20.1	0.003
3	Tap slag	0.230	4.68	4.27	1.74	0.42	1.13	0.503	19.1	7.7	19.0	0.024
3	Bar	0.163	2.51	2.39	0.89	0.38	1.19	0.480	15.7	5.7	20.4	0.025

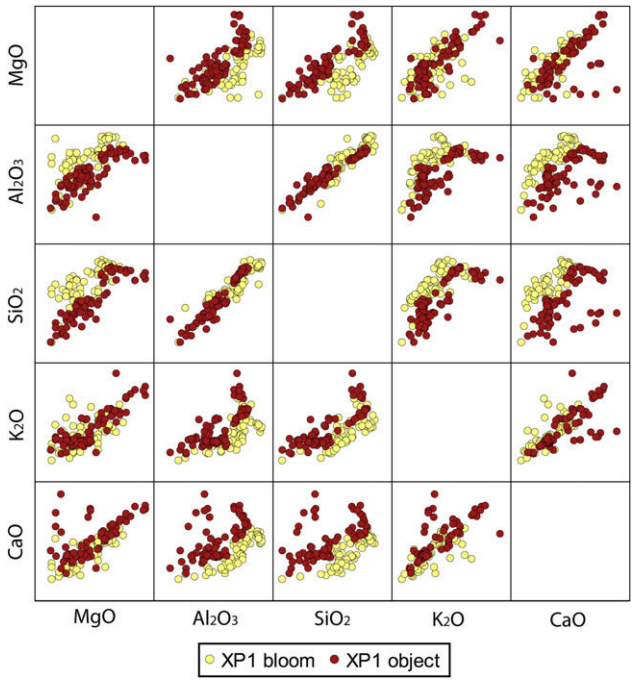

Fig. 5. Bivariate scatterplot matrix showing non-reduced compounds (NRC) in SI in iron objects from experiment 1 compared to the bloom from the same smelt.

K_2O/MgO ratios ($t(152) = -2.14$, $p = 0.83$). Conversely, there was a significant difference between the MgO/CaO ($t(152) = 2.824$, $p = 0.005$) and K_2O/CaO ratios ($t(152) = 4.655$, $p = 0.000$), which are higher in the object SI. SiO_2/MgO, SiO_2/CaO and SiO_2/K_2O are higher in the bloom SI, which is probably related to a higher fuel ash contribution in the smithed objects. Again, this finding highlights the significant contribution of fuel ash to the chemical composition of SI. Although this has previously been noted for smelting slag (Crew, 2000; Paynter, 2006), its relevance in the study of object SI has not been emphasised before. This pattern is also seen when comparing the above ratios in the slag and SI in the bloom and iron bars from Snorup (Høst-Madsen and Buchwald, 1999).

4.3. SI in objects and metallurgical slag

The next stage of our data analysis focused on the comparison between the SI in objects and the relevant slag produced during smelting and smithing. As noted before, several types of slag formed during the smelting process, namely ceramic-rich slag, bloom slag, and tap slag. The ceramic-rich slag was rather heterogeneous in composition, and no clear patterns could be identified when comparing SI in objects to this slag type. On the contrary, a good correlation was apparent for NRC ratios between the object SI and the bloom slag, but our small sample size does not allow for generalisations. Although this type of slag is rarely identified in archaeological contexts, it has been reported in some instances (e.g. Buchwald, 2005, p. 168), and future finds of similar slag might be targeted specifically for potential SI provenance studies.

Of much more archaeological relevance are, however, tap slags, as these are far more abundant in archaeometallurgical sites, more frequently analysed, and therefore more susceptible to comparisons in object SI studies. Tap slag is typically rather homogeneous in chemical composition, given that this composition is constrained by the process requirements: only slag with a relatively low melting point and low viscosity will flow out of the furnace. As a result, when plotted in bivariate plots, chemical compositions of tap slag tend to form rather tight clusters (Rehren et al., 2007, Fig. 2), as opposed to the linear scatters displayed by object SI. Thus a visual comparison of NRC ratios between slag and SI becomes more difficult, and it becomes more important to combine visual approaches with statistical analyses.

For both experiments 1 and 3, the best matches between NRC of tap slag and SI visually appear to be in the plot of K_2O/MgO. In addition, for experiment 3, a good match is noticeable for MnO/SiO_2 (Fig. 6). The statistical significance of these observations was demonstrated through *t*-tests (Table 9). The *t*-tests carried out with the MnO/SiO_2 values for slag and SI from XP1 are less convincing

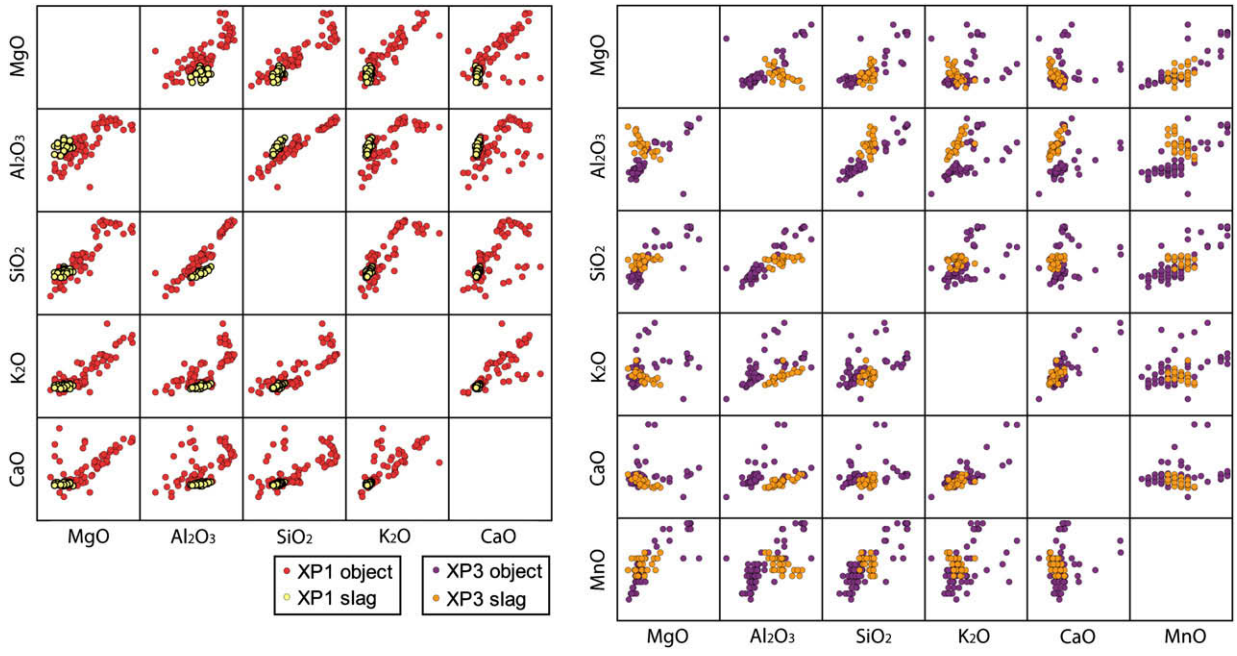

Fig. 6. Bivariate scatterplot matrix showing NRC in SI in iron objects compared to tap slag from the same smelt, for both experiments 1 and 3.

(Table 9). This is most likely due to the low levels of MnO in the slag and SI (Tables 3 and 5), around the detection limits of the EDS, which results in less reliable data. The plots of K_2O/MgO against MnO/SiO_2 in Fig. 7 clearly demonstrate the differences between XP1 and XP3, and the correspondence between tap slag and SI for each experiment. It is worth remembering that these were also the most diagnostic NRC ratios to differentiate between objects from different production systems (see Section 4.1). Thus, these ratios would not only allow us to group objects but also, potentially, to ascribe these groups to different smelting slag and therefore smelting systems. Such attribution should be performed with caution, however, since, as noted above, the alkali and alkali earth oxide concentrations may be significantly affected by the fuel ash contribution, and fuel may furthermore differ between smelter and smith. While MnO is clearly an ore-related compound, all the other compounds mentioned may be subject to fluctuations in fuel composition. From a visual inspection of Fig. 6, it might also appear that the MgO/CaO and K_2O/CaO ratios are comparable between the SI and the relevant slag in each experiment. However, such patterns could not be validated through *t*-tests and will therefore not be discussed further.

Perhaps more important is the fact that, for both experiments, the Al_2O_3/SiO_2, Al_2O_3/MgO, Al_2O_3/K_2O and Al_2O_3/CaO ratios are lower in the objects than in the tap smelting slag of reference. This relationship was confirmed when a *t*-test was carried out on the slag and object SI from experiments 1 and 3, where there was always a significant difference in these ratios, with the average ratio always being lower in the objects (Table 9). The likely explanation for this pattern lies in the sand flux used during smithing (and the subsequent SiO_2 enrichment in the SI; see also Dillmann and L'Héritier, 2007), and the longer contact with the fuel experienced by the objects in the smithing hearth (resulting in the MgO and K_2O enrichment in the SI). As noticed in the object microstructures, there was enough contact with the fuel in the smithing hearth to allow for carburisation to occur in the bars from XP1 and XP3, and the billet from XP2, which highlights the important role played by the fuel in the chemistry of slag and SI.

A similar pattern is noted in the data presented by Høst-Madsen and Buchwald (1999) for Iron Age Snorup, where SI compositions for a number of iron bars are compared to those of smelting slags. Based on other microstructural and chemical data, these authors concluded that only one of the bars analysed could be positively ascribed to the suspected smelting slag. Significantly, this is the only bar where all the above SI ratios are higher than in the smelting slag. Thus, although more experimental data will be needed to substantiate this claim, it would appear that the Al_2O_3/SiO_2, Al_2O_3/MgO, Al_2O_3/K_2O and Al_2O_3/CaO ratios may be useful as a "negative criteria" to reject potential source candidates for an archaeological object: should these ratios be higher in the object SI than in the suspected slag, then the candidate may be rejected.

A final comparison was attempted between the composition of SI and that of the relevant smithing slags. It turned out, however, that smithing slags are too heterogeneous to be characterised on the basis of NRC ratios, and therefore no significant patterns could be identified. It is only on a qualitative basis that the relevant bars can be ascribed to their smithing slags of reference – namely, in our experiments, by the presence/absence of MnO.

5. Archaeological case study: early iron in the Near East

Excavations at Tell Hammeh, Jordan, have revealed extensive remains of iron smelting and primary smithing operations dated to the 10th century BC (930 Cal BC, by AMS radiocarbon dating). Complex layering of the industrial debris at the site suggests that smelting activity was carried out on a seasonal basis. Systematic

Table 9
Results (*t*-value (*t*), degrees of freedom (df) and probability (*p*)) from a series of *t*-tests for average NRC ratios for slag and SI of the experimental material.

Slag	Sample	Al_2O_3/SiO_2			Al_2O_3/MgO			Al_2O_3/K_2O			Al_2O_3/CaO			K_2O/MgO			MnO/SiO_2			K_2O/CaO			MgO/CaO		
		t	df	*p*	*t*	df	*p*	*t*	df	*p*	*t*	df	*p*	*t*	df	*p*	*t*	df	*p*	*t*	df	*p*	*t*	df	*p*
XP1	XP1 Billet	18.7	64.8	0.00	8.2	45.4	0.00	8.1	57.8	0.00	5.1	44.7	0.00	1.2	58.9	0.23	1.7	46.0	0.09	0.0	47.1	0.97	−3.3	55.9	0.00
	XP1 Bar	12.4	59.8	0.00	9.9	53.0	0.00	20.6	72.7	0.00	14.5	65.4	0.00	−0.8	71.7	0.43	−2.1	68.6	0.04	−6.7	52.0	0.00	−3.3	62.6	0.00
	XP2 Billet	15.0	54.2	0.00	6.3	71.1	0.00	17.8	71.9	0.00	31.5	58.5	0.00	−0.7	66.4	0.50	1.0	53.4	0.31	5.3	69.1	0.00	0.1	56.4	0.94
	XP3 Bar	18.3	90.0	0.00	18.3	31.7	0.00	22.1	87.1	0.00	17.5	84.0	0.00	8.5	66.8	0.00	−20.2	82.6	0.00	0.9	74.5	0.37	−3.9	64.0	0.00
XP3	XP1 Billet	6.6	36.3	0.00	−2.9	37.2	0.01	4.1	64.3	0.00	3.2	49.9	0.00	−3.9	66.8	0.00	23.4	41.5	0.00	1.1	66.1	0.28	5.6	33.3	0.00
	XP1 Bar	6.6	62.8	0.00	−1.3	41.2	0.21	14.4	70.8	0.00	10.5	72.5	0.00	−6.6	53.9	0.00	16.8	62.1	0.00	−4.3	72.8	0.00	5.5	33.7	0.00
	XP2 Billet	9.4	69.1	0.00	−2.6	58.8	0.01	11.4	67.1	0.00	21.4	46.6	0.00	−5.6	70.5	0.00	21.9	47.2	0.00	4.5	46.2	0.00	6.4	35.8	0.00
	XP3 Bar	9.2	54.2	0.00	3.4	30.3	0.00	15.2	74.0	0.00	13.9	91.4	0.00	−0.4	44.6	0.71	−0.6	72.8	0.52	1.8	86.5	0.08	0.3	91.5	0.80

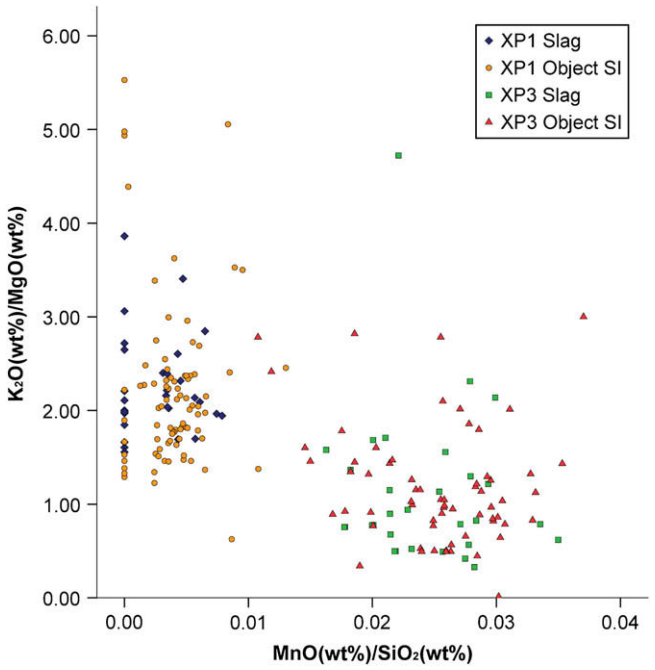

Fig. 7. Plot of selected NRC for experiments 1 and 3, showing the differences between the two smelting systems and a good correspondence between object SI and the relevant smelting slag in both cases.

excavations were also carried out at the secondary smithing site of Tell Beth-Shemesh, located in Israel, 75 km southwest of Hammeh. AMS radiocarbon dates of c. 900 Cal BC indicate that the smithing activity at this workshop was contemporaneous with the smelting site. The assemblage of artefacts recovered included metallurgical debris such as technical ceramics, smithing hearth bottom slag and hammerscale. Research has shown that the smithing workshop operated regularly and at a considerable scale, possibly supplying the large town (Veldhuijzen, 2005a; Veldhuijzen and Rehren, 2007).

The locations of the two sites are very different, with the smelting site of Tell Hammeh located near the raw materials required, and the smithing site of Tel Beth-Shemesh located near the consumer. Interestingly, however, the tuyères at both sites are virtually identical in shape and fabric, which seems to indicate that there may have been contact between smelters and smiths. This is particularly suggestive given the peculiar square section of the tuyères, for which there is no technical explanation, and which may therefore represent a cultural/social link. The largely uniform shape and size of the tuyères suggests coherent organisation of production, and is strongly indicative of standardisation and possibly that the two sites were socio-ethnically linked (Veldhuijzen, 2005a,b). In spite of these apparent links, it remained to be tested whether the metal smithed in Beth-Shemesh was supplied by the smelters at Tell Hammeh.

Previous analytical work and mass balance calculations have shown that a substantial segment of the tuyères melted and contributed to the slag formation during the smelting episodes at Hammeh (Veldhuijzen, 2005a; Veldhuijzen and Rehren, 2007). This further stresses the pertinence of comparing object SI to smelting slags rather than ores, in order to account for this ceramic signature. The Hammeh tap slag is characterised by very high CaO (~10%) and relatively low FeO levels (~50%), together with significant concentrations of SO_3 and MnO (slag analyses by (P)ED-XRF and SEM–EDS, see Veldhuijzen, 2005a; Veldhuijzen and Rehren, 2007).

Very few iron artefacts were found at Hammeh, and none of them in direct stratigraphic association with the smelting remains. The only Hammeh object included in this research (HA97 69) was an arrowhead found in a layer stratigraphically above the smelting remains, and therefore likely to date to a later period. In comparison, over 26 artefacts and 100 fragments of iron were found in the Beth-Shemesh smithy. Included in this assemblage were billets, arrowheads, knives and numerous iron strips. Two out of the three billets found in Beth-Shemesh were selected, as this artefact type was deemed to best represent the iron used at the smithing workshop. The third billet was too badly corroded for analysis. The remaining samples were chosen from the best preserved artefacts to reflect the different artefact types at the site, i.e. arrowheads,

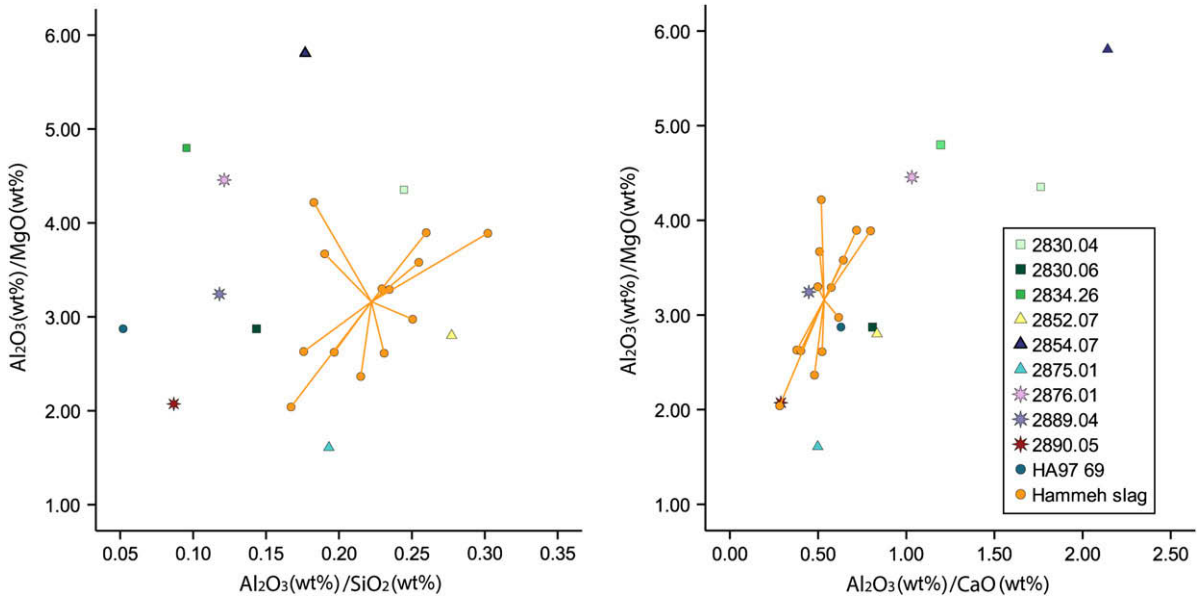

Fig. 8. Plot of selected NRC ratios of SI in the iron objects from Hammeh and Beth-Shemesh, compared to tap slag from Hammeh. According to the criteria derived from the experiments, objects with SI "consistent" with the Hammeh slag should plot in the bottom left quarter defined by the Hammeh slag group (i.e. these ratios should be lower in the objects than in the slag).

Table 10
Results (*t*-value (*t*), degrees of freedom (df) and probability (*p*)) from a series of *t*-tests for average NRC ratios for the Hammeh smelting slag and the SI in archaeological objects from Hammeh and Beth-Shemesh.

Sample	Al_2O_3/SiO_2			Al_2O_3/MgO			Al_2O_3/K_2O			Al_2O_3/CaO			K_2O/MgO			MnO/SiO_2		
	t	df	*p*	*t*	df	*p*	*t*	df	*p*	*t*	df	*p*	*t*	df	*p*	*t*	df	*p*
2834.26	10.1	16.5	0.00	−4.5	12.0	0.00	5.6	14.6	0.00	−14.0	21.0	0.00	−7.7	9.1	0.00	8.8	15.0	0.00
2854.07	11.5	28.0	0.00	−2.2	56.9	0.03	1.2	48.2	0.25	−3.7	56.5	0.00	−3.3	47.6	0.00	9.6	14.0	0.00
HA97 69	5.3	33.7	0.00	−1.8	53.2	0.08	−0.3	65.7	0.78	−3.6	53.6	0.00	−3.8	54.1	0.00	9.6	14.0	0.00
2876.01	0.5	18.1	0.61	−2.9	15.9	0.01	−2.7	15.3	0.02	−3.3	15.1	0.01	−0.7	15.4	0.52	9.6	14.1	0.00
2889.04	6.3	29.7	0.00	−1.4	38.7	0.16	4.9	16.7	0.00	−0.7	49.9	0.47	−2.5	37.3	0.02	9.1	14.2	0.00
2830.06	1.9	25.4	0.06	−1.0	25.4	0.32	−0.5	20.2	0.63	−2.7	19.3	0.01	−2.2	22.2	0.04	9.4	14.2	0.00
2830.04	−2.0	31.9	0.05	−4.3	29.2	0.00	−1.9	18.6	0.07	−2.5	18.0	0.02	−0.4	31.3	0.68	9.5	14.1	0.00
2852.07	−5.4	22.2	0.00	0.6	15.7	0.57	−1.3	29.8	0.20	−6.2	29.6	0.00	1.2	29.5	0.24	5.1	18.7	0.00
2875.01	1.1	27.9	0.26	5.9	15.5	0.00	0.6	24.2	0.54	−0.7	27.5	0.48	3.8	25.6	0.00	9.3	14.9	0.00
2890.05	7.9	30.3	0.00	−0.1	23.4	0.93	−1.1	17.2	0.28	−1.0	19.1	0.35	0.4	24.1	0.67	9.3	14.5	0.00

knives and a blade fragment. The results of the SI analyses in all of these objects were compared to those from the Hammeh smelting slag.

Due to the large number of objects and individual measurements involved, it is not possible to plot every single SI composition in the graphs, and average NRC ratios for each object are used instead. However, visual observations were tested statistically for significance. Firstly, based on the previous findings from the experimental material, should the Beth-Shemesh objects originate from Hammeh, the Al_2O_3/SiO_2, Al_2O_3/MgO, Al_2O_3/K_2O and Al_2O_3/CaO ratios in their SI should not be higher than in the suspected smelting slag (as per trends observed in Section 4.3, Fig. 6 and Table 9). As shown in Fig. 8, there is a relatively broad scatter of SI compositions, suggesting that several iron smelters were supplying Beth-Shemesh. However, it would appear that a few objects are in fact consistent with the Hammeh smelting slag (i.e. they seem to have equal or lower ratios). These patterns were validated for objects 2889.04, 2875.01 and 2890.05, which all had ratios lower than, or equal to, those in the slag (Table 10).

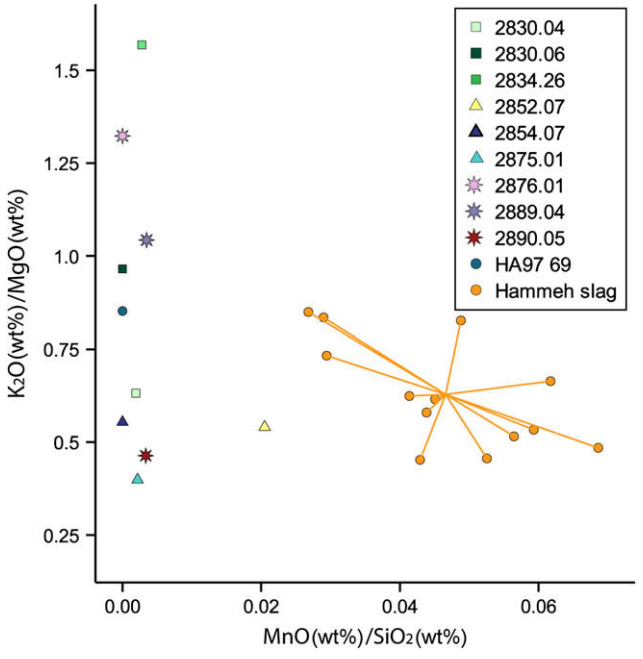

Fig. 9. Plot of selected NRC ratios of SI in the iron objects from Hammeh and Beth-Shemesh compared to tap slag from Hammeh. According to the criteria derived from the experiments, objects with SI "consistent" with the Hammeh slag should plot together with the slag group (i.e. they should have the same ratios).

The next test involved comparing the K_2O/MgO and MnO/SiO_2 ratios, which, based on the experimental data (Section 4.3), should be the same for the object SI and the relevant smelting slag. Here, both the graph (Fig. 9) and the *t*-tests (Table 10) show that the average K_2O/MgO ratio in some object SI would seem comparable to that ratio in the slag, but the MnO/SiO_2 does not show any matches. Out of the three objects singled out above as potentially consistent with the Hammeh smelting system, only 2890.05 shows a K_2O/MgO ratio that is statistically similar to that in the slag, and none of them shows an analogous MnO/SiO_2 ratio. The relatively high MnO levels in the Hammeh slag make this system potentially comparable to our XP3, and thus the very different MnO/SiO_2 ratios between slag and SI lead us think that not even object 2890.05 would originate from the Hammeh system. However, we must acknowledge that this sample shows the closest match: so long as our experiment-derived criteria remain provisional and awaiting further verification, this conclusion will have to remain provisional too.

Finally, it is worth highlighting that not even the iron object found at Hammeh (HA97 69) appears completely consistent with the smelting slag from the site, as it shows a higher Al_2O_3/CaO and statistically different K_2O/MgO and MnO/SiO_2 ratios. However, as noted above, this object is later than the smelting slag and thus, although it might have been made locally, it is unlikely to derive from the smelting system documented archaeologically at Hammeh.

6. Summary and conclusion

The main goal of this research was to employ data from experimental assemblages to contribute to iron provenance studies based on slag inclusions. Given the relatively small number of experimental assemblages studied so far, the patterns observed can only be regarded as provisional. However, it is worth highlighting some of our findings, hoping that they will encourage further work on experimental assemblages, and eventually facilitate provenance studies based on SI.

A first point to be stressed is that the chemical signature of smelting slag and SI is not necessarily dominated by the chemical composition of the ore alone. Other factors such as melting technical ceramics, fuel ash and potential fluxes, in addition to variable furnace operating parameters, play a crucial role in slag formation and thus in the slag composition. A particularly striking case is exemplified in experiments 1 and 2, where a rich ore was employed, and the chemical signature of the resulting slag was dominated by fuel ash compounds. Owing to this, SI studies seem better suited for comparisons between objects and contemporary smelting slag, thus relating objects to specific smelting systems rather than to overall geological bodies. This should not rule out

completely the possibility of ascribing archaeological objects to broad geographic regions based on SI compositions, but such attributions will only be possible for ores with very diagnostic chemical signatures, and where the archaeological and/or historical evidence allows for a reasonable assumption.

There is a wide variability in the composition of individual SI in iron artefacts, and even in relatively unprocessed iron objects such as blooms. However, the ratios between NRC remain broadly constant for most of the SI within a given iron object. On this basis, the comparison of NRC ratios is confirmed as a simple and useful strategy for the grouping and potential provenancing of iron objects based on SI (Dillmann and L'Héritier, 2007; Paynter, 2006). Having said this, it is important to note that the Al_2O_3/SiO_2 ratio, previously used to group iron objects from different regions (Buchwald and Wivel, 1998), is not enough as a discerning criterion by itself; our experiments show that objects produced in completely different smelting systems had comparable Al_2O_3/SiO_2 ratios, due to varying contributions of ore, ceramic and fuel ash diluting any specific chemical signature. Furthermore, observations made on graphic data plots should always be tested for statistical significance. Here we attempted to use bivariate plots in order to assess their potential. We found that, although they are useful for initial data exploration, they may also be misleading as one may see trends in the data that are not statistically significant. Future studies may benefit from the use of multivariate statistics with compositional values or NRC ratios. However, such statistical approaches will only be particularly effective once we have amassed a body of experimental data allowing us to discern the most reliable compounds or NRC to be considered in provenancing attempts.

In the experiments reported here, MgO/K_2O and SiO_2/MnO were shown as the most useful ratios in identifying objects from the same smelting system, and differentiating these from others. These ratios were also consistent between smelting slag and object SI from the same system, and it is thus suggested that they may be useful in future provenance studies based on SI. It should be noted that further ratios may be of use in relevant case studies. In particular, TiO_2, like MnO, is an NRC typically low in clay and fuel ash – hence it is likely to be constrained mostly by the ore chemistry. Thus, this may be a useful discerning compound when studying smelting systems or SI containing high levels of this oxide. Furthermore, a critical difficulty lies in the fact that some ratios, including those with K_2O, MgO and CaO, may be affected by variable fuel ash contributions. Thus, if the charcoal employed differs significantly from smelter to smith, or even between smiths, these chemical markers may be distorted too. Future studies should therefore collect and analyse charcoal samples from smelting or smithing activities wherever possible. Analyses of trace elements in SI, for example employing LA-ICP-MS, will no doubt yield a larger number of NRC data that may enable more convincing groupings and comparisons between object SI and smelting slags. However, these analytical systems are still scarcely available compared to less expensive SEM–EDS. As with isotopic studies, some compromises will have to be made to accommodate cost, the generation of useful data, and the development of analytical methods and protocols that may be used by many researchers.

Another important pattern noted in all experiments was that the Al_2O_3/SiO_2, Al_2O_3/MgO, Al_2O_3/K_2O and Al_2O_3/CaO ratios were lower in the object SI than in the tap smelting slag of reference. As discussed above, this indicates that not only potential fluxes, but also the fuel used in the smithing hearth, have an impact on the chemical composition of object SI. Based on this realisation, however, it is suggested that these ratios could be useful in comparisons between archaeological objects and slag where a provenance link is suspected: if the Al_2O_3/SiO_2, Al_2O_3/MgO, Al_2O_3/K_2O and Al_2O_3/CaO ratios appear higher in the object SI, then they are unlikely to originate from the suspected smelting system.

In our case study, the criteria derived from the experiments were applied to compare between the Iron Age smelting slag from Tell Hammeh (Jordan), and the SI in objects from the contemporaneous Beth-Shemesh smithy (Israel). Although a few object SI did meet some of the above criteria, in particular sample 2890.05, none of them fully satisfied the patterns derived from the experiments. Thus the provisional results suggest that, in spite of other links apparent between the sites, the iron smithed in Beth-Shemesh was not from the smelting site of Hammeh.

Innumerable slags and iron objects resulting from experimental reconstructions lie under-researched in storage facilities. It is hoped that this study will encourage others to exploit their informative potential, in order to test the validity of the trends observed and discussed here.

Acknowledgements

We are grateful to the Amgueddfa Cymru, the National Museum of Wales, and many people who helped during the smelting experiments. Thanks also go to the staff and students at the UCL Institute of Archaeology, for all their expertise and support during the analysis. We further gratefully acknowledge to the AHRC, who funded the MSc research on which this article is based, and to the Leverhulme Trust, for their funding towards the Hammeh and Beth-Shemesh research.

We are also indebted to the Scientific Directors of the *Deir 'Alla Regional Project* (Dr Zeidan Kafafi and Dr Gerrit van der Kooij) and the Scientific Directors of the Tel Beth-Shemesh Excavations (Dr Shlomo Bunimovitz and Dr Zvi Lederman) for allowing us to analyse iron artefacts and slag from Hammeh and Beth-Shemesh. Finally, our thanks go to the two anonymous referees and Sarah Paynter for all their helpful suggestions and comments, and especially to Mike Charlton, whose insightful remarks considerably improved the paper.

References

Allen, J.R.L., 1988. Chemical compositional patterns in Romano-British bloomery slags from the wetlands of the Severn Estuary. Historical Metallurgy 22, 81–86.

Bachmann, H.G., 1982. The Identification of Slags from Archaeological Sites. In: Occasional Publication 6. Institute of Archaeology, London.

Blakelock, E.S., 2007. Slag Inclusions and the Quest for Provenance: Slag and Slag Inclusions from Iron Smelting Experiments and their Application in Slag Inclusion Analyses of Artefacts from Tell Hammeh, Jordan and Tel Beth-Shemesh, Israel. Unpublished Masters Dissertation, UCL Institute of Archaeology.

Buchwald, V.F., 2005. Iron and Steel in Ancient Times. Historisk-filosofiske Skrifter. Det Kongelige Danske Videnskabernes Selskab, Copenhagen.

Buchwald, V.F., Wivel, H., 1998. Slag analysis as a method for the characterization and provenancing of ancient iron objects. Materials Characterization 40, 73–96.

Bullas, S.G., 1995. Identifying your local slag. The use of quantitative methods and microstructure analysis in determining the provenance of British bloomery slags from the late Iron Age to the end of the roman occupation. In: Huggett, J., Ryan, N. (Eds.), Computer Applications and Quantitative Methods in Archaeology. BAR International Series, 600, pp. 95–99. Oxford.

Coustures, M.P., Béziat, D., Tollon, F., Domergue, C., Long, L., Rebiscoul, A., 2003. The use of trace element analysis of entrapped slag inclusions to establish ore–bar iron links: examples from two Gallo-Roman ironworking sites in France (Les Martys, Montagne Noire and Les Ferrys, Loiret). Archaeometry 45, 599–613.

Crew, P., 1991. The experimental production of Prehistoric bar iron. Historical Metallurgy 25, 21–36.

Crew, P., 2000. The influence of clay and charcoal ash on bloomery slags. In: Tizzoni, C.C., Tizzoni, M. (Eds.), Il Ferro nelle Alpi, Atti del Convegno/Iron in the Alps. Proceedings of the Conference, pp. 38–48.

Dillmann, P., L'Héritier, M., 2007. Slag inclusion analyses for studying ferrous alloys employed in French medieval buildings: supply of materials and diffusion of smelting processes. Journal of Archaeological Science 34, 1810–1823.

Hedges, R.E.M., Salter, C.J., 1979. Source determination of iron currency bars through analysis of the slag inclusions. Archaeometry 21, 161–175.

Høst-Madsen, L., Buchwald, V.F., 1999. The characterization and provenancing of ore, slag and iron from the iron age settlements at Snorup. Historical Metallurgy 33, 57–67.

McDonnell, G., 1986. The Classification of Early Ironworking Slags. Unpublished Ph.D., University of Aston.
McDonnell, G., 1987. The study of early iron smelting residues. In: Scott, B.G., Cleere, H., Tylecote, R.F. (Eds.), The Crafts of the Blacksmith. Ulster Museum/UISPP Comité pour la Sidérurgie Ancienne, Belfast, pp. 47–52.
McDonnell, G., 1991. A model for the formation of smithing slags. Materialy Archeologiczne 26, 23–26.
Paynter, S., 2006. Regional variations in bloomery smelting slag of the Iron Age and Romano-British periods. Archaeometry 48, 271–292.
Pleiner, R., 2000. Iron in Archaeology: the European Bloomery Smelters. Archaeologický Ústav Avěr.
Pleiner, R., 2006. Iron in Archaeology: Early European Blacksmiths. Archaeologický Ústav Avěr.
Rehren, Th., Charlton, M., Chirikure, S., Humphris, J., Ige, A., Veldhuijzen, H.A., 2007. Decisions set in slag: the human factor in african iron smelting. In: La Niece, S., Hook, D.R., Craddock, P.T. (Eds.), Metals and Mines – Studies in Archaeometallurgy. Archetype, British Museum, London, pp. 211–218.
Rostoker, W., Bronson, B., 1990. Pre-Industrial Iron: Its Technology and Ethnology. Archaeomaterials Monograph No. 1 Philadelphia.
Serneels, V., Perret, S., 2003. Quantification of smithing activities based on the investigation of slag and other material remains. In: Proceedings of the International Conference Archaeometallurgy in Europe. Associazione Italiana di Metallurgia, Milano, pp. 469–479.
Tylecote, R.F., 1986. The Prehistory of Metallurgy in the British Isles. Institute of Metals, London.
Veldhuijzen, H.A., 2005a. Early Iron Production in the Levant. Smelting and Smithing at Early 1st Millennium BC Tell Hammeh, Jordan and Tel Beth-Shemesh, Israel. Unpublished Ph.D., UCL Institute of Archaeology.
Veldhuijzen, H.A., 2005b. Technical ceramics in early iron smelting. The role of ceramics in the early first millennium BC iron production at Tell Hammeh (az-Zarqa), Jordan. In: Prudencio, I., Dias, I., Waerenborgh, J.C. (Eds.), Understanding People Through Their Pottery: Proceedings of the Seventh European Meeting on Ancient Ceramics (EMAC '03). Instituto Português de Arqueologia (IPA), Lisboa, pp. 295–302.
Veldhuijzen, H.A., Rehren, Th., 2007. Slags and the city: Early iron production at Tell Hammeh, Jordan, and Tel Beth-Shemesh, Israel. In: La Niece, S., Hook, D.R., Craddock, P.T. (Eds.), Metals and Mines – Studies in Archaeometallurgy. Archetype, British Museum, London, pp. 189–201.